Heterogeneity and Anisotropy of Earth's Inner Core

Arwen Deuss

Bullard Labs, Department of Earth Sciences, University of Cambridge, Cambridge CB3 0EZ, United Kingdom; email: afd28@cam.ac.uk

Annu. Rev. Earth Planet. Sci. 2014. 42:103–26

First published online as a Review in Advance on February 5, 2014

The *Annual Review of Earth and Planetary Sciences* is online at earth.annualreviews.org

This article's doi:
10.1146/annurev-earth-060313-054658

Keywords

seismology, body waves, free oscillations, mineralogy, dynamics, iron, solidification

Abstract

Seismic observations provide strong evidence that Earth's inner core is anisotropic, with larger velocity in the polar than in the equatorial direction. The top 60–80 km of the inner core is isotropic; evidence for an innermost inner core is less compelling. The anisotropy is most likely due to alignment of hcp (hexagonal close-packed) iron crystals, aligned either during solidification or by deformation afterward. The existence of hemispherical variations used to be controversial, but there is now strong evidence from both seismic body wave and normal mode observations, showing stronger anisotropy, less attenuation, and a lower isotropic velocity in the western hemisphere. Two mechanisms have been proposed to explain the hemispherical pattern: either (*a*) inner core translation, wherein one hemisphere is melting and the other is solidifying, or (*b*) thermochemical convection in the outer core, leading to different solidification conditions at the inner core boundary. Neither is (yet) able to explain all seismically observed features, and a combination of different mechanisms is probably required.

1. INTRODUCTION

The core, comprising the innermost parts of Earth, is one of the most dynamic regions of our planet. The inner core is solid, surrounded by an outer core of a liquid iron alloy. Inner core solidification releases latent heat that, combined with motions in the fluid outer core, drives the geodynamo, generating Earth's magnetic field (Buffett et al. 1992, Gubbins et al. 2003). Solidification of the inner core also supplies some of the heat that drives mantle convection and subsequently plate tectonics at Earth's surface. Thus, the inner core is key to understanding the inner workings of our planet, and details of its heterogeneity and anisotropy may provide constraints on Earth's thermal and compositional structure.

No direct samples can be taken of Earth's outer and inner core, so our knowledge of its heterogeneity and anisotropy relies on seismology, which is the only technique that can "see through" Earth and map its velocity and density structure. Ray theoretical studies using short-period body waves provide the most commonly used seismological data. These have led to the discovery of a range of features in the inner core, including anisotropy (e.g., Morelli et al. 1986), hemispherical variations (e.g., Tanaka & Hamaguchi 1997), and the existence of an innermost inner core (e.g., Ishii & Dziewonski 2002). Some of these structures have also been seen using long-period normal mode observations (e.g., Woodhouse et al. 1986, Deuss et al. 2010).

These exciting, but also confusing, observations of seismological inner core structure have led to numerous fundamental questions regarding the thermal and compositional structure. Many of these questions still remain unanswered: What causes inner core anisotropy? Which high-pressure phase of iron is stable in the inner core? How do we generate hemispheres? And does inner core structure relate to the magnetic field? Here, I give an overview of the major discoveries in inner core anisotropy and heterogeneity that have been made in the past 30 years or so, and discuss dynamical and mineralogical implications of the observations.

2. SEISMOLOGICAL OBSERVATION METHODS

There are two different types of seismological data that are used to observe the structure of the inner core: (*a*) body waves at the short-period range (frequency approximately 1 Hz) and (*b*) normal modes at the long-period range (frequency less than 10 mHz). Ideally, we would like to see the same structures in both data types, or at least understand why a structure would only be seen using one data type.

2.1. Body Waves

Most studies of the inner core are performed using short-period compressional body waves at frequencies between 0.5 and 1.5 Hz (a dominant period of 1 s), making the waves visible with sharp and clear onsets. Due to their short-period nature, body waves provide information on small-scale structure and the properties of discontinuities, including the inner core boundary and potential additional discontinuities inside the inner core. The main shortcoming of body waves is that arrival times and amplitudes for inner core velocity and attenuation models need to be calculated using ray theoretical methods, which require approximations. Also, body waves provide information only on velocity and attenuation structure, not on density. Another limitation is that body waves sample just a few small regions of the inner core due to uneven station and earthquake distribution.

The compressional body wave of interest is called PKIKP, where P denotes travel in the mantle, K means travel through the outer core, and I means travel through the inner core (**Figure 1**). When

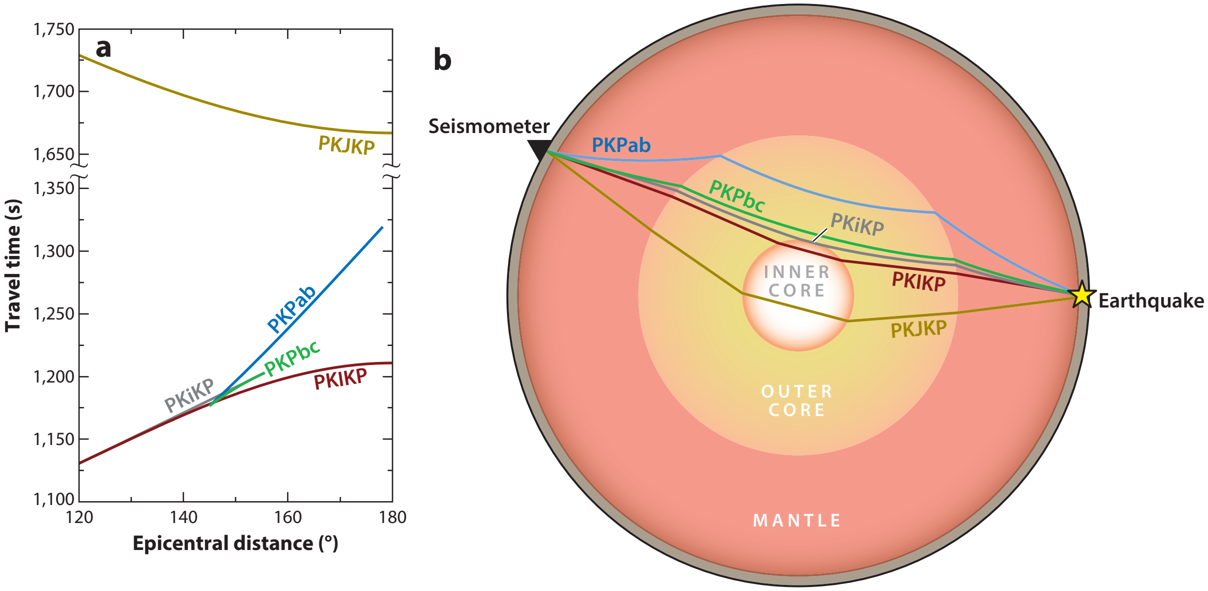

Figure 1

(*a*) Travel time curves for inner core compressional wave PKIKP; its reference phases PKPbc, PKPab, and PKiKP; and inner core shear wave PKJKP. (*b*) Corresponding ray paths through Earth, for an epicentral distance of 150°.

this phase is studied on its own, corrections for mantle structure are required (Morelli et al. 1986, Shearer 1994, Su & Dziewonski 1995, Li & Cormier 2002, Lythgoe et al. 2013). Alternatively, PKIKP is studied in combination with a reference phase, which only travels the mantle and outer core. At epicentral distance ranges of 130–143°, PKiKP, which reflects off the inner core boundary (hence i), is used as reference phase (e.g., Wen & Niu 2002, Cao & Romanowicz 2004, Cormier 2007, Waszek et al. 2011, Waszek & Deuss 2011, Cormier et al. 2011). PKIKP and PKiKP have very similar paths, and by taking the differential travel time between PKIKP and PKiKP we remove the influence of the mantle and crust. PKPbc is used as a reference phase at 146.5–156.5° (e.g., Shearer & Toy 1991; Creager 1992; Bhattacharyya et al. 1993; Souriau & Roudil 1995; Song & Richards 1996; Souriau & Romanowicz 1996, 1997; Creager 1997; Tanaka & Hamaguchi 1997; Song 2000; Song & Li 2000; Collier & Helffrich 2001; Tseng et al. 2001; Isse & Nakanishi 2002; Garcia et al. 2006; Lindner et al. 2010; Irving & Deuss 2011a), and PKPab is used at even larger epicentral distances, though the paths start diverging quite significantly and corrections for crust and mantle structure are again required (Vinnik et al. 1994; McSweeney et al. 1997; Creager 1999, 2000; Song & Xu 2002; Garcia et al. 2006; Kazama et al. 2008; Irving & Deuss 2011a).

PKIKP and its reference phases are easily observed in earthquakes with body wave magnitude m_b greater than 5.5; seismologists have been successful in making data sets containing several hundreds to thousands of PKIKP measurements (e.g., Shearer & Toy 1991; Creager 1992, 1999; Vinnik et al. 1994; Song & Helmberger 1995; Tanaka & Hamaguchi 1997; Wen & Niu 2002; Cao & Romanowicz 2004; Garcia et al. 2006; Irving & Deuss 2011a; Waszek & Deuss 2011). When PKIKP is used on its own, the onset is usually measured, which is the best indicator of its actual arrival time. More elaborate techniques, such as cross-correlation, have been used between PKIKP and its reference phases. This works well for PKPbc, which has the same waveform as PKIKP. For PKPab, a Hilbert transform must be applied (e.g., Vinnik et al. 1994), and PKiKP has opposite polarity due to its reflection at the inner core boundary.

In principle, it should also be possible to study the inner core with shear waves, such as PKJKP (**Figure 1**). Shear waves exist only in solid materials, and thus PKJKP has to pass the fluid outer core as a compressional wave and then change to a shear wave at the inner core boundary (called J). The conversion between compressional and shear wave energy at the inner core boundary causes a lot of energy loss, resulting in a small amplitude and making inner core shear waves very difficult to observe. In addition, strong inner core shear attenuation makes the amplitude even smaller (e.g., Deuss et al. 2000, Andrews et al. 2006, Shearer et al. 2011).

2.2. Normal Modes

Normal modes are whole-Earth oscillations and are excited by large earthquakes (e.g., Dahlen & Tromp 1998). They are standing waves along the surface and radius of Earth and are studied at the opposite end of the frequency spectrum, at periods larger than 100 s or frequencies less than 10 mHz. At these periods, normal modes sensitive to the inner core are observed as individual peaks in the frequency spectrum. The spectrum is calculated by taking seismograms several days long and then performing a simple Fourier transformation from time to frequency domain. Spheroidal modes are the long-period analog of P-SV body waves or Rayleigh surface waves. They are denoted ${}_nS_l$, where n is the overtone number and l is the angular order; modes sensitive to the inner core usually have high n and low l. Each mode ${}_nS_l$ consists of $2l+1$ different surface oscillation patterns, called singlets, all of which have the same frequency in a spherically symmetric nonrotating Earth (i.e., they are degenerate). However, anisotropy and heterogeneity split the singlets into different frequencies (removing the degeneracy), observations of which can be used to determine inner core anisotropy and heterogeneity. Inner core–sensitive modes are mostly studied on their own (i.e., the self-coupling approximation), though when two modes are close in frequency, cross-coupling occurs. This has been taken into account in recent studies, leading to new ways to image inner core structure (Deuss & Woodhouse 2001, Irving et al. 2009, Deuss et al. 2011).

The advantage of normal modes is that they are sensitive to density in addition to velocity and attenuation and therefore are the only data type to tell us about density in the inner core. They are not limited by earthquake and receiver locations and thus are able to provide global constraints on inner core structure. In addition, the theory to calculate normal mode spectra for a model of the inner core is in principle exact (Woodhouse & Deuss 2007), so unlike with ray theory for body waves there is no need for approximations. Amplitude effects are fully calculated, so the normal modes should be able to give better constraints on attenuation than do the body waves.

3. DISCOVERY AND SOLIDITY

Earth's outer core was discovered by Oldham (1906), and Gutenberg proposed the core to be fluid by identifying a shadow zone in which neither compressional nor shear waves were observed. When Lehmann (1936) did observe a compressional wave in the core shadow zone, she suggested the existence of an inner core inside the fluid outer core from which the wave had to be reflected. She also suggested that the inner core would most likely be solid, even though at that time there was no direct evidence.

3.1. Solidity

Birch (1940) provided mineralogical evidence for solidity of the inner core by showing that the pressure in the inner core is so high that the solidus must be crossed. Then, Bullen (1946) hypothesized that the bulk modulus in Earth would only change smoothly as a function of depth.

Consequently, the sharp increase in compressional velocity from the outer to the inner core must be due solely to an increase in shear modulus in the inner core. Birch (1952) used this idea to calculate inner core shear wave velocity to be 3.5 km/s, which is remarkably close to the currently accepted value of 3.6 km/s from normal mode observations (Dziewonski & Anderson 1981, Deuss 2008).

To prove that the inner core is solid, seismological evidence is needed. Normal mode observations provided the first such evidence in the 1970s (Dziewonski & Gilbert 1971). However, direct evidence in the form of inner core shear wave observations, or PKJKP, was still lacking. The amplitude of PKJKP is five times smaller than that of PKIKP because of the inefficient conversion from compressional to shear wave energy at the inner core boundary (Bullen 1951); the additional effect of attenuation was thought to make it impossible to observe PKJKP at all (Doornbos 1974).

Julian et al. (1972) claimed to have observed PKJKP, but they found an inner core shear wave velocity of 2.95 km/s, which is in disagreement with normal mode constraints. Making use of larger data sets and stacking seismograms for deep and large earthquakes, investigators finally made unequivocal observations of PKJKP in the early 2000s (Deuss et al. 2000, Cao et al. 2005, Wookey & Helffrich 2008). Because of the long history of unsuccessful observations of PKJKP, it is important that claims are justified by using the fluid inner core test (Deuss et al. 2000), which casts doubt on an earlier observation by Okal & Cansi (1998). Calculations of synthetic seismograms for models with a solid and fluid inner core, including all other mantle and outer core phases arriving in the PKJKP time window, are compared and must show that the claimed PKJKP is visible only in the solid inner core calculations and is absent in the fluid inner core equivalent. One recent PKJKP observation showed some evidence of shear wave splitting, requiring 1% inner core shear wave anisotropy (Wookey & Helffrich 2008), though this observation is at surprisingly short period and has very large amplitude, requiring inner core shear attenuation to be zero as opposed to the strong shear attenuation found in normal mode studies. The few inner core shear wave observations available are likely due to favorable focusing in exceptional events and may not be representative of average inner core structure (Shearer et al. 2011).

3.2. Inner Core Boundary

That PKJKP can be observed requires the inner core boundary to be sharp enough for energy to be converted from compression to shear. The density jump at the inner core boundary provides information on the difference in composition between the outer and inner core and may be related to the solidification process of the inner core. Masters & Gubbins (2003) determined the density jump by fitting normal mode frequencies and found a value of 0.82 ± 0.18 g/cm^3. Body wave studies, fitting the amplitude ratio between PKiKP and PcP, give values as low as 0.52 ± 0.24 g/cm^3 in some studies (Koper & Pyle 2004, Koper & Dombrovskaya 2005), an upper bound of 1.1 g/cm^3 (Tkalčić et al. 2009), and even values as large as 1.35–1.66 g/cm^3 in an older study (Souriau & Souriau 1989).

The wide range found in body wave studies most likely occurs because PKiKP and PcP are very difficult to observe in the epicentral distance range required for these measurements. The lowest reported values would cause problems for observing PKJKP; given that there are now a number of PKJKP observations, these values are probably too low. Some studies have proposed the existence of a mushy layer containing a mixture of fluid and solid at the top of the inner core (Fearn et al. 1981). The thickness of the mushy layer depends on the details of the solidification process and the amount of convection within the layer. In light of the PKJKP observations, it seems unlikely that the mushy layer is much thicker than a few kilometers.

The inner core boundary is expected to be nearly spherical and does not contain much topography (Souriau & Souriau 1989, Buffett 1997). However, studies using PKiKP have found scattering at the inner core boundary (Vidale & Earle 2000, Cormier & Li 2002, Krasnoshchekov et al. 2005), and some have even suggested the existence of small-scale topography (Cao et al. 2007). At the base of the outer core, a region with lower compressional velocity, called the F layer, is found (e.g., Song & Helmberger 1995, Yu et al. 2005). This layer is probably related to the solidification of the inner core, preferentially partitioning the light elements in the outer core and reducing compressional velocity.

4. ANISOTROPY

4.1. Velocity Anisotropy

Inner core anisotropy was discovered in the 1980s with waves in the north–south or polar direction traveling several seconds faster than waves in the east–west or equatorial direction, an observation that also provided further proof for inner core solidity. The strength of the observation was that it was seen in both short-period body waves (Poupinet et al. 1983, Morelli et al. 1986) and long-period normal modes (Woodhouse et al. 1986).

4.1.1. Body wave observations. Body wave evidence comes from PKIKP observations as a function of the angle ζ between Earth's rotation axis (assumed to be the symmetry axis of the anisotropy) and the direction of the PKIKP ray in the inner core. Paths with ζ less than 35° are defined as polar paths, and those with ζ greater than 35° are called equatorial paths. Assuming cylindrical anisotropy with Earth's rotation axis as symmetry axis, the body wave travel time measurements are modeled following Creager (1999):

$$\frac{\delta t}{t} = \frac{\delta v}{v} = \mathrm{a} + \mathrm{b}\cos^2\zeta + \mathrm{c}\cos^4\zeta, \tag{1}$$

where δt is the travel time perturbation, t is the travel time in the inner core, δv is the compressional velocity perturbation, and v is the reference compressional inner core velocity. The constant a is the perturbation in equatorial velocity, and b + c quantifies the amount of anisotropy, defined as the difference in travel time residual (or velocity), between the purely polar ($\zeta = 0°$) and equatorial ($\zeta = 90°$) directions.

PKiKP-PKIKP differential travel times, which are sensitive to the top 100 km of the inner core, show little evidence for variation of δt with ζ (**Figure 2**), suggesting an isotropic layer at the top of the inner core. Waves traveling deeper than approximately 60 km show a small amount of anisotropy, limiting the thickness of the isotropic layer to 50–80 km (Song & Helmberger 1995, Ouzounis & Creager 2001, Garcia 2002, Yu & Wen 2007, Waszek & Deuss 2011). Some studies using PKPbc-PKIKP or PKIKP have found thicker isotropic layers, varying from 100 to 250 km (Su & Dziewonski 1995, Song & Helmberger 1998, Creager 2000, Garcia & Souriau 2000, Isse & Nakanishi 2002, Song & Xu 2002, Sun & Song 2008), but these body waves travel deeper than 150 km in the inner core and therefore cannot uniquely determine the structure in the upper 150 km.

The deeper parts of the inner core are sampled by PKPbc-PKIKP and PKPab-PKIKP differential times, which show strong variations of δt with ζ (**Figures 2** and **3**). The equatorial direction ($\zeta = 90°$) is slow, and is perpendicular to the fast polar direction ($\zeta = 0°$), requiring anisotropy of 3–4% all the way down to the center of the inner core (Creager 1992, Vinnik et al. 1994, McSweeney et al. 1997, Creager 1999, Garcia & Souriau 2000, Sun & Song 2008, Irving & Deuss 2011a). The deepest parts of the inner core are studied by using PKIKP on its own. Absolute travel time studies using PKIKP arrival times from the International Seismological Centre catalog show weaker anisotropy of only 1–3% (Morelli et al. 1986, Shearer & Toy 1991, Shearer 1994,

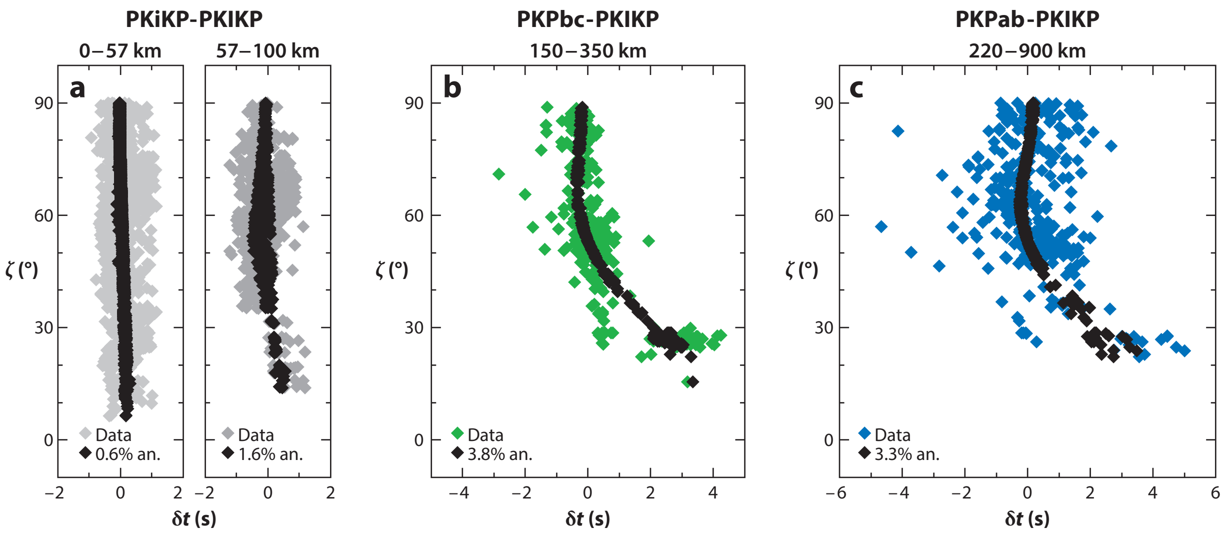

Figure 2

Body wave observations of inner core anisotropy. (*a*) PKiKP-PKIKP differential times: observations (*gray*) and predictions for 0.6% and 1.6% anisotropy (*black*). (*b*) PKPbc-PKIKP: observations (*green*) and predictions for 3.8% anisotropy (*black*). (*c*) PKPab-PKIKP: observations (*blue*) and predictions for 3.3% anisotropy (*black*). The amount of anisotropy increases for waves that travel deeper in to the inner core; there is an isotropic layer (less than 1% anisotropy) in the top 57 km, just below the inner core boundary, and more than 3% anisotropy in the deeper parts. Data are from Irving & Deuss (2011a) and Waszek & Deuss (2011). Abbreviation: an., anisotropy.

Su & Dziewonski 1995), possibly because the more strongly anomalous arrivals are missed by the operator picking the data. Handpicked PKIKP arrival time studies show stronger anisotropy in agreement with the differential travel times (Cao & Romanowicz 2007, Lythgoe et al. 2013).

4.1.2. Normal mode observations. Anisotropy is also seen in normal modes. Observed splitting function observations for modes that are sensitive to the inner core show strong zonal splitting (Woodhouse et al. 1986, He & Tromp 1996, Durek & Romanowicz 1999, Deuss et al. 2013), which is seen as positive frequency anomalies near the poles and a negative frequency anomaly along the equator (**Figure 4**). When calculating the splitting function for a model of inner core anisotropy, in addition to mantle structure from model S40RTS (Ritsema et al. 2011) and crustal structure from CRUST5.1 (Mooney et al. 1998), we can reproduce the zonal splitting. However, if only mantle and crustal structure are included in the prediction, then positive anomalies are found in the "ring around the Pacific" instead, which is the expected signature of mantle structure.

Normal mode splitting function measurements have been inverted to obtain models of inner core anisotropy, parameterized in terms of α and β (related to twice the velocity difference between polar and equatorial directions for compressional and shear waves, respectively) and a third parameter γ (related to waves traveling in other directions) (i.e., Woodhouse et al. 1986). The values for α (3.5% to 6.7%) and β (0.7% to 1.7%) are quite well constrained, but γ varies strongly between the different models (−2.7% to 2.3%) (Woodhouse et al. 1986, Tromp 1995, Durek & Romanowicz 1999, Beghein & Trampert 2003). In comparison with the body waves, normal mode models display 1.7–3.3% compressional anisotropy, which is somewhat smaller than required by the body waves. With the limited number of PKJKP observations, normal mode observations remain the main source of information on shear wave anisotropy, requiring approximately 0.35–0.85%.

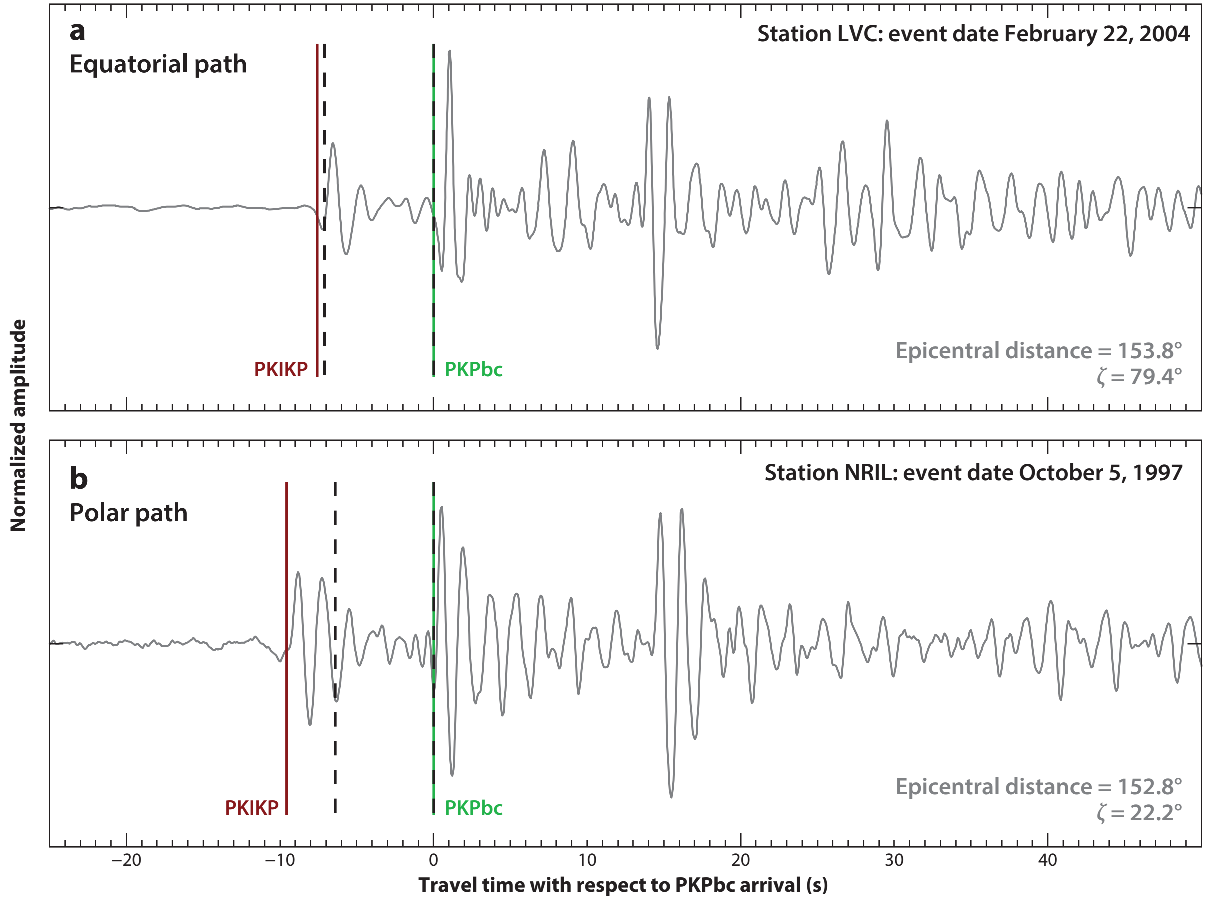

Figure 3

Example seismograms for (*a*) an equatorial path, with inner core wave PKIKP (*red solid line*) and outer core wave PKPbc (*green solid line*) both arriving close to the predicted times (*black dashed lines*) for a 1D isotropic reference model and (*b*) a polar path, with inner core wave PKIKP arriving early, leading to a positive differential PKPbc-PKIKP time, indicating a faster velocity and inner core anisotropy. After Irving & Deuss (2011a).

Normal modes preferentially place the strongest anisotropy near the top of the inner core, which is where they have the largest sensitivity; this is in contradiction with the body waves, which require an isotropic layer of at least 60–80 km at the top. However, it is possible to fit the normal modes with the imposition of an isotropic layer at the top (Durek & Romanowicz 1999, Irving & Deuss 2011b), thus reconciling the normal modes and body waves.

4.2. Attenuation Anisotropy

Body wave studies also find attenuation anisotropy, wherein the waves traveling in the polar direction are more attenuated than waves traveling in the equatorial direction. The attenuation anisotropy is clearly visible in the amplitudes of PKIKP/PKPbc and PKIKP/PKPab, which are systematically lower for polar than for equatorial paths (Souriau & Romanowicz 1996, 1997; Oreshin & Vinnik 2004). The amplitudes of PKIKP/PKiKP also vary between polar and equatorial

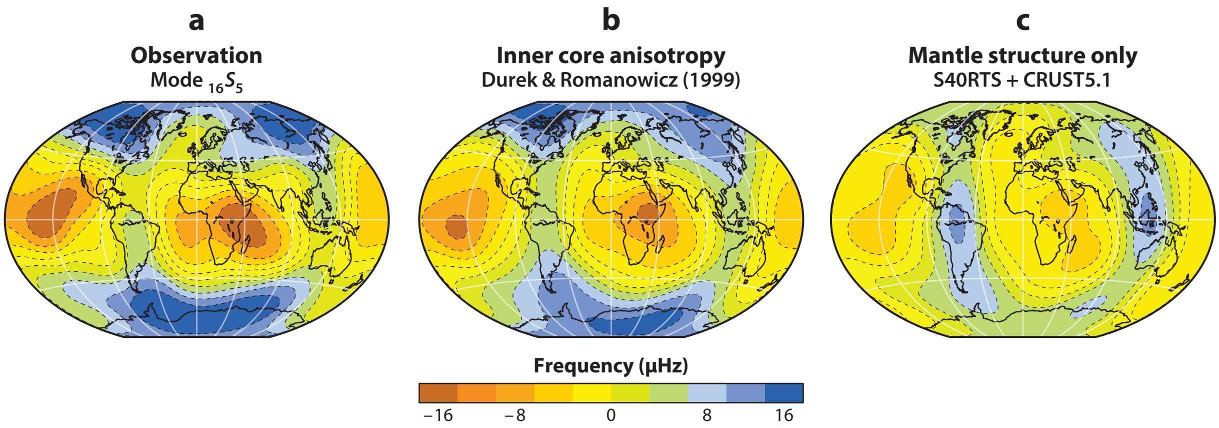

Figure 4

Normal mode observations of inner core anisotropy. (*a*) Splitting function observation for mode $_{16}S_5$. (*b*) Prediction for inner core anisotropy and mantle structure. (*c*) Prediction for mantle and crustal structure only. Modified from Deuss et al. (2010).

paths in some studies (Yu & Wen 2006a) but not in others (Cao & Romanowicz 2004). The problem is that the observed variation in PKIKP/PKiKP amplitude with ζ may be due to variations in velocity structure at the inner core boundary instead, and thus would not require any attenuation anisotropy in the top 100 km of the inner core (Waszek & Deuss 2013).

The varying results found with body waves, especially for PKiKP/PKIKP, show that modeling body wave amplitudes is complicated by the ray theoretical approximations. It may actually be impossible to separate the amplitude effects due to 3D structure, source geometry, and attenuation. Normal modes, in contrast, separate easily into an elastic (i.e., velocity) and an anelastic (i.e., attenuation) contribution (Masters et al. 2000). Measurements of anelastic splitting functions also find strong zonal splitting, confirming attenuation anisotropy using normal mode observations; in agreement with the body wave observations, the direction of fast velocity is more strongly attenuating (Mäkinen & Deuss 2013).

4.3. Innermost Inner Core

Some body wave and normal mode studies have suggested the existence of an innermost inner core. Using PKIKP observations, Ishii & Dziewonski (2002, 2003), Cao & Romanowicz (2007), Niu & Chen (2008), and Sun & Song (2008) have found that anisotropy changes its signature at a radius of 300 to 500 km, at which point the slowest direction is no longer perpendicular to the fastest direction but is instead at an angle of 45–55° from Earth's rotation axis. Using normal mode splitting functions, Beghein & Trampert (2003) found that the anisotropy completely changed sign at a radius of 400 km, such that the polar direction is slow and the equatorial direction is fast. Some studies have also seen a difference in attenuation for the innermost inner core (Cormier & Li 2002, Li & Cormier 2002, Cormier & Stroujkova 2005).

However, the evidence for an innermost inner core is not compelling. Using body waves, Cormier & Stroujkova (2005) and Garcia et al. (2006) failed to find any reflections from a potential discontinuity at the top of the innermost inner core. Moreover, a recent body wave study showed that the innermost inner core may be an artifact of averaging over the two hemispheres (see below). They found that the data are better fit by a model with hemispheres down to the center of the inner core without the need for an innermost inner core (Lythgoe et al. 2013).

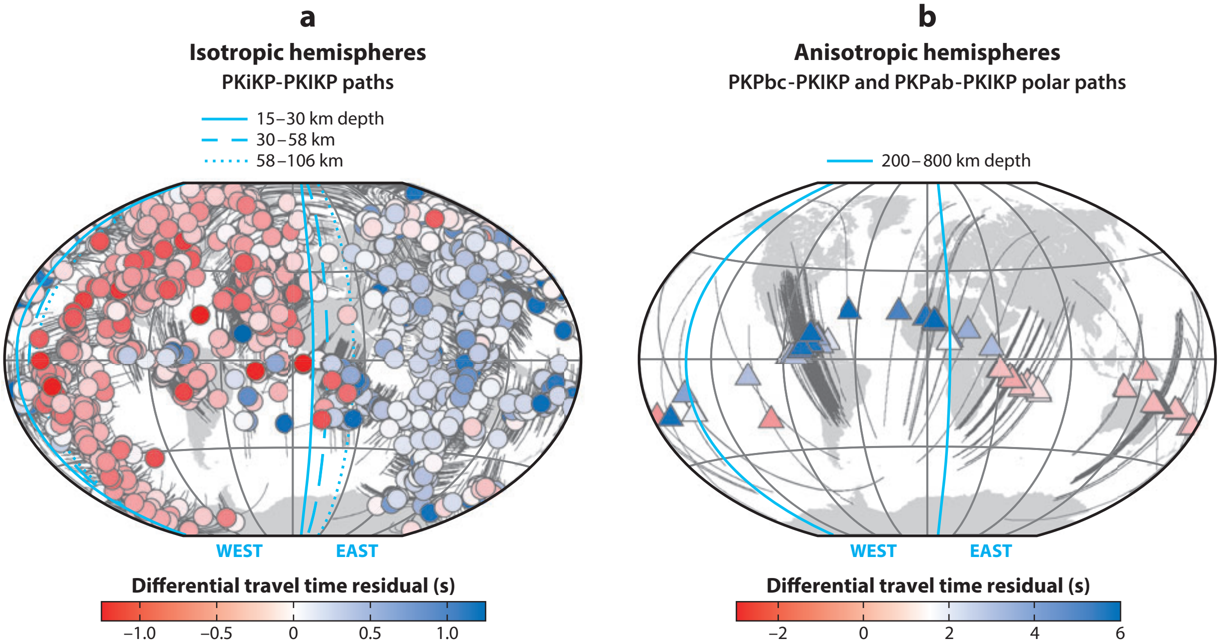

Figure 5

Body wave observations of hemispherical variations. (*a*) PKiKP-PKIKP observations sampling the top 100 km, showing difference in equatorial paths, which suggests isotropic variations. (*b*) PKPbc-PKIKP and PKPab-PKIKP polar observations sampling deeper than 150 km, showing anomalous anisotropic paths in the west but not in the east. Light blue lines indicate hemisphere boundaries. Data are from Irving & Deuss (2011a) and Waszek & Deuss (2011).

5. HEMISPHERICAL VARIATION

Early body wave studies of inner core anisotropy found the symmetry axis to be tilted with respect to Earth's rotation axis, in order to explain variation of the polar paths' arrival times with turning longitude in the inner core (Shearer & Toy 1991, Su & Dziewonski 1995, Song & Richards 1996, McSweeney et al. 1997). More recently, it was shown that the inner core displays lateral variations instead (**Figure 5**): The western hemisphere is more strongly anisotropic and has a lower isotropic velocity than the eastern hemisphere (Tanaka & Hamaguchi 1997). The hemispherical variations removed the need for a tilted anisotropy axis and provide a better fit to the body wave data (Irving & Deuss 2011a). For a while it was argued that the data do not require hemispherical variations and are fit just as well by simple homogeneous models (e.g., Ishii et al. 2002a,b). However, the hemispherical variations are now seen using both body waves and normal modes (e.g., Tanaka & Hamaguchi 1997, Deuss et al. 2010), and I believe that evidence for their existence is robust.

5.1. Isotropic Structure

Very clear evidence for hemispherical variations is seen in the isotropic velocity variation for the top 100 km of the inner core, which is imaged using equatorial PKiKP-PKIKP paths (Niu & Wen 2001, Garcia 2002, Waszek & Deuss 2011). Taking hemispheres into account, there is still an isotropic layer of up to 60–80 km thickness at the top of the inner core in the western hemisphere. In addition, the western hemisphere is approximately 1.5% slower than the eastern hemisphere in the top 100 km. Equatorial PKiKP-PKIKP paths have good global coverage and therefore also provide the tightest constraints on the hemisphere boundary locations. The eastern boundary varies from 11°E to 60°E and the western boundary from −161°W to −180°W in the different studies. When the data are divided into three depth layers, the boundary between the two hemispheres is sharp (i.e., it appears over a narrow longitudinal range) and actually dips eastward as a function of depth (Waszek et al. 2011). A dipping hemisphere boundary also explains the range seen among the studies, as the boundary location will vary with the depth being sampled.

The PKIKP/PKiKP and PKPbc/PKIKP amplitude ratios in the top few hundred kilometers of the inner core also display a hemispherical difference: The eastern hemisphere has lower amplitudes and is thus more strongly attenuating ($Q \approx 160$–300) than the western hemisphere ($Q \approx 330$–600) (Tseng et al. 2001; Wen & Niu 2002; Cao & Romanowicz 2004; Ivan et al. 2006; Yu & Wen 2006a,b; Cormier 2007; Yu & Wen 2007; Waszek & Deuss 2013). The isotropic hemispherical difference in both velocity and attenuation has not (yet) been imaged with normal modes.

5.2. Anisotropic Structure

A hemispherical difference in anisotropy was initially discovered using body wave observations (Tanaka & Hamaguchi 1997). Recently, normal mode splitting function observations have confirmed the existence of strong anisotropy in the east and weaker anisotropy in the west (Deuss et al. 2010).

5.2.1. Body wave observations. The difference in isotropic velocity between the hemispheres becomes smaller (less than 0.5%) for the PKPbc-PKIKP and PKPab-PKIKP paths, which sample deeper than 150 km in the inner core (Irving & Deuss 2011a, Tanaka 2012). Here, the main difference between the east and west hemispheres is in the polar paths, where strongly anomalous paths are only seen in the western hemisphere, which suggests that the west is anisotropic while the east is isotropic (Tanaka & Hamaguchi 1997, Creager 1999, Irving & Deuss 2011a). Using these data, the eastern boundary is found at longitudes from 14°E to 50°E and the western boundary at 160°E to −95°W (Tanaka & Hamaguchi 1997, Creager 1999, Garcia & Souriau 2000, Oreshin & Vinnik 2004, Irving & Deuss 2011a, Lythgoe et al. 2013). The boundaries between the hemispheres vary strongly among the different studies, due to the limited global distribution of polar paths. The other problem is that the data are dominated by polar paths from earthquakes in the South Sandwich Islands region traveling to stations in Alaska, which only sample the western hemisphere (Tkalčić 2010).

The part of the western hemisphere below the isotropic layer is now found to have up to 5% anisotropy, whereas the eastern hemisphere has less than 0.7% compressional anisotropy (Creager 1999, Garcia & Souriau 2000, Ouzounis & Creager 2001, Niu & Wen 2002, Sun & Song 2008, Irving & Deuss 2011a, Waszek & Deuss 2011). Some studies suggest that no anisotropy in the east is required at all (Lythgoe et al. 2013). The amount of anisotropy is variable between the studies, possibly due to the different definitions of the hemisphere boundaries.

5.2.2. Normal mode observations. Recently the hemispherical difference in anisotropy has also been observed using normal mode cross-coupling observations (Deuss et al. 2010), which are not limited by the earthquake locations. Although some studies highlighted problems with observing hemispherical differences using body waves, the fact that they are now also seen using normal mode data makes the evidence compelling. Observations of isolated modes are sensitive to even-degree structure and therefore provide information only on the average anisotropy of the two hemispheres. Hemispheres are odd-degree structure, which can only be observed by studying

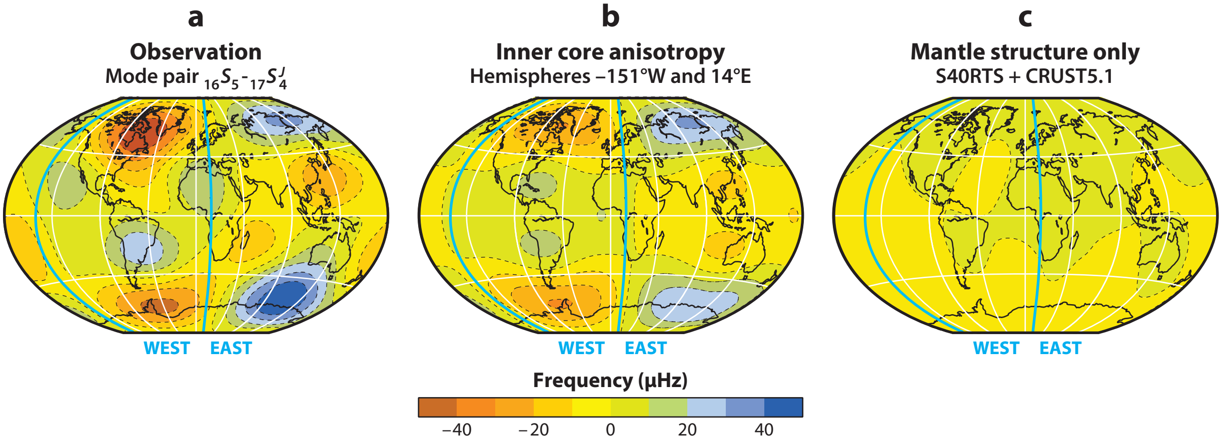

Figure 6

Normal mode observations of hemispherical variations. (*a*) Splitting function for mode pair ${}_{16}S_5$-${}_{17}S_4^J$, with ${}_{17}S_4^J$ being an inner core confined mode. (*b*) Predicted splitting function for inner core hemispherical anisotropy and mantle structure, with boundaries at −151°W and 14°E, matching the observation. (*c*) Prediction for mantle and crustal structure only. Light blue lines indicate hemisphere boundaries. Modified from Deuss et al. (2010).

cross-coupled pairs of normal modes ${}_nS_l$-${}_{n'}S_{l'}$ that differ in angular order (i.e., $l - l'$) by an odd number.

Deuss et al. (2010) made the first observations of cross-coupled inner core splitting and found that the observations matched the expectations for hemispherical variation in anisotropy—the west is more strongly anisotropic, in agreement with the body wave observations. Moreover, for most of the pairs, one of the modes is an inner core confined mode that is uniquely sensitive to the inner core, thus proving that the hemispherical difference cannot be due to mantle or outer core structure as had been suggested before (Romanowicz & Breger 2000). Even more convincingly, the strongest anisotropy is found in exactly the same location under North and South America as in the body wave studies without using data from South Sandwich Islands events (**Figure 6**).

6. SUPERROTATION

Inner core superrotation was first suggested from geodynamo modeling, which predicted the inner core to rotate with respect to the crust and mantle in either prograde (i.e., faster) or retrograde (i.e., slower) direction, depending on the assumed toroidal magnetic field in the outer core (Gubbins 1981, Glatzmaier & Roberts 1995, Aurnou et al. 1998). Alternatively, the inner core may be gravitationally locked with the mantle, depending on the inner core viscosity, in which case the inner core would not be able to superrotate (Buffett 1997). Seismologists searched and found evidence for inner core superrotation by observing that PKPbc-PKIKP differential travel times systematically changed over a period of several decades (Song & Richards 1996, Su et al. 1996). Normal mode studies, however, show an ambiguous picture, finding faster and slower rotation rates with quite large uncertainties, and therefore cannot (yet) distinguish between superrotation and gravitational locking (Sharrock & Woodhouse 1998, Laske & Masters 1999). It is not surprising that the different methods that are used to determine the superrotation rate give such varying numbers because each technique has its own limitation. For example, the seismic body wave data that is more than two decades old is more noisy and event locations are less well determined, making it difficult to measure superrotation rates back in time. A similar problem occurs for the normal

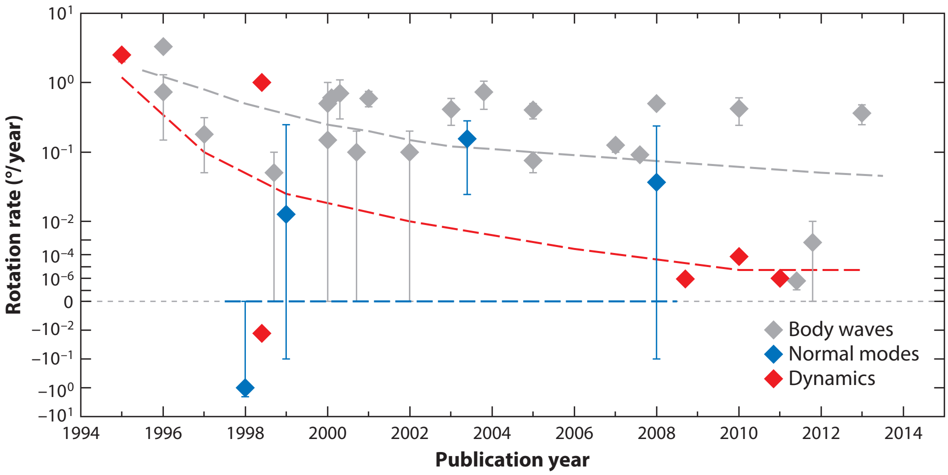

Figure 7

Inner core superrotation rate as a function of year of publication; gray diamonds denote body wave observations (Song & Richards 1996, Su et al. 1996, Creager 1997, Poupinet et al. 2000, Souriau 1998, Song 2000, Song & Li 2000, Souriau & Poupinet 2000, Vidale et al. 2000, Collier & Helffrich 2001, Isse & Nakanishi 2002, Li & Richards 2003, Xu & Song 2003, Vidale & Earle 2005, Zhang et al. 2005, Cao et al. 2007, Song & Poupinet 2007, Song & Dai 2008, Zhang et al. 2008, Lindner et al. 2010, Waszek et al. 2011, Tkalčić et al. 2013), blue diamonds show normal mode observations (Sharrock & Woodhouse 1998; Laske & Masters 1999, 2003; Tomiyama & Oda 2008), and red diamonds are calculations from geodynamo modeling and coupling between mantle and inner core (Glatzmaier & Roberts 1995, Aurnou et al. 1998, Aubert et al. 2008, Dumberry 2010, Aubert & Dumberry 2011).

mode data, for which there are fewer than 10 seismic stations available in the 1970s and early 1980s. Thus, a few more decades of data will ideally be needed to make robust measurements. In addition, the geodynamo calculations are performed for fluid dynamical conditions that are still quite far from values expected for the outer core, making it difficult to predict inner core superrotation rates.

Interestingly, the numbers quoted from body wave observations for the amount of superrotation (**Figure 7**) have gone down over the years from the initial reports of 1–3°/year (Song & Richards 1996, Su et al. 1996) to smaller recent values of less than 0.5°/year (e.g., Song & Poupinet 2007, Lindner et al. 2010, Tkalčić et al. 2013). Several body wave studies have even argued that there is no inner core superrotation at all (Souriau 1998, Poupinet et al. 2000, Souriau & Poupinet 2000, Isse & Nakanishi 2002, Mäkinen & Deuss 2011). In particular, a recent study argued that closely spaced stations in Alaska show opposite rotation rates, which is not consistent with a solid-body rotation (Mäkinen & Deuss 2011).

The superrotation rates predicted from geodynamical calculations have gone down in size even more dramatically, from up to 3°/year (Glatzmaier & Roberts 1995) to the most recent values of 1°/Myr when gravitational locking and constraints from changes in length of day are taken into account (Dumberry 2010, Dumberry & Mound 2010, Aubert & Dumberry 2011). Assuming that the hemispherical variations are frozen in as the inner core grows over time, Waszek et al. (2011) used body wave observations of the dipping boundaries between the hemispheres to estimate an inner core superrotation rate of 0.1–1°/Myr. This number is in close agreement with small rotation rates from Aubert & Dumberry (2011); the faster reported rotation rates from body waves would then be due instead to a faster decadal inner core oscillation (e.g., Tkalčić et al. 2013).

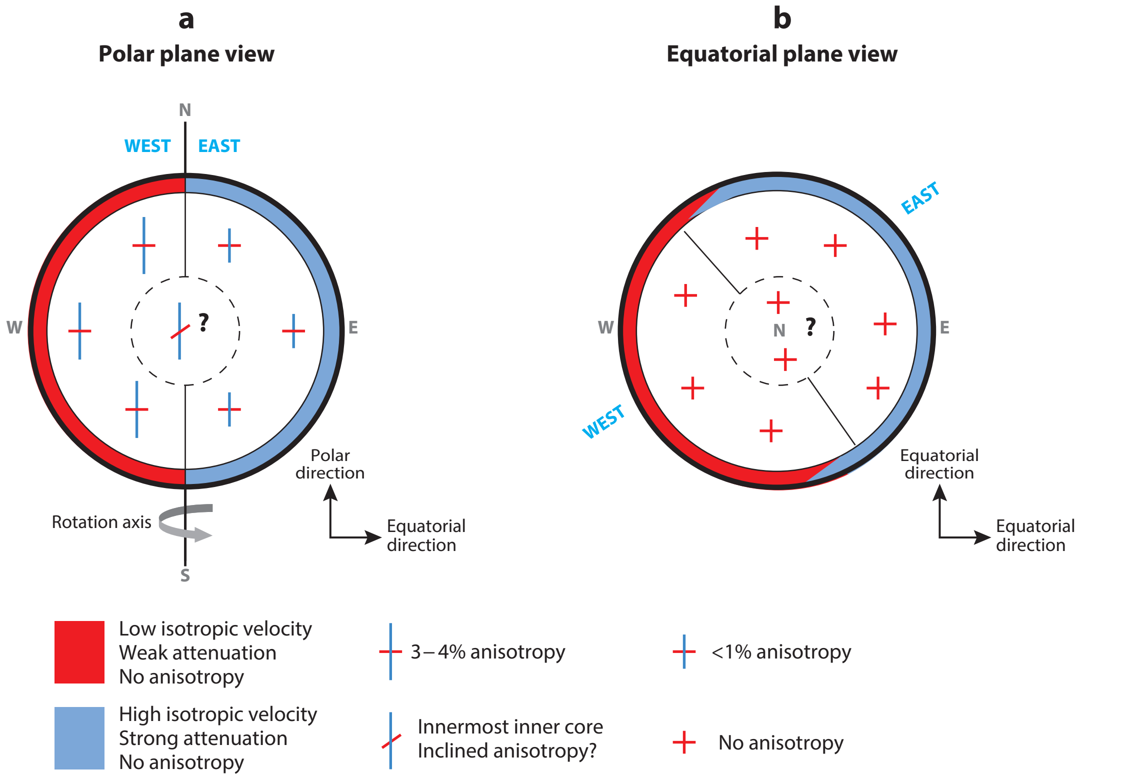

Figure 8

Schematic overview of the seismically observed structure in the inner core in (*a*) the polar plane, which shows hemispherical differences including strong anisotropy in the west, and (*b*) the equatorial plane, in which there is no anisotropy, but the hemispherical difference in isotropic velocity and attenuation in the top layer is still visible.

7. DYNAMICAL AND MINERALOGICAL INTERPRETATION

The range of structures observed in the inner core is schematically summarized in terms of the two different hemispheres (**Figure 8**). The top 60–80 km of the inner core is isotropic, with strong anisotropy in the deeper parts of the western hemisphere. The eastern hemisphere, in contrast, contains almost no anisotropy, has a larger isotropic velocity, and is more strongly attenuating than the western hemisphere. The proposed innermost inner core may be an artifact, and superrotation is most likely quite small, if it exists at all. Ideally, we would like to explain all of the seismically observed features using known mineralogical and dynamical properties of the inner core.

7.1. Mineralogy

The stable phase of iron is well known at ambient pressure and temperatures from both experiments and ab initio calculations, forming the bcc (body-centered cubic) phase and then transforming to the fcc (face-centered cubic) phase with increased temperature. At increased pressure, the hcp (hexagonal close-packed) phase is formed. Ab initio calculations have been used to determine the properties of iron at simultaneous high temperature and high pressure, and hcp is the firm favorite for pure iron (Vočadlo et al. 2000, 2003a). Taking into account that the inner core also needs to accommodate a few percent of light elements (Jephcoat & Olsen 1987, Stixrude et al. 1997), ab initio calculations suggest that the bcc phase (Belonoshko et al. 2003, Vočadlo et al. 2003b, Dubrovinsky et al. 2007, Côté et al. 2008), or even the fcc phase (Vočadlo et al. 2008), might become stable instead.

Recently, experimentalists managed to reach inner core temperature and pressure simultaneously in the diamond anvil cell; they found only hcp to be stable for pure iron or iron with nickel and/or silicon (Tateno et al. 2010, 2012; Sakai et al. 2011). Thus, bcc and fcc are very unlikely to be stable in the inner core, and I will focus on hcp in the remaining discussion.

7.2. Anisotropy

Anisotropy is due to either shape-preferred orientation (SPO) or lattice-preferred orientation (LPO). SPO by alignment of fluid inclusion has been proposed by Singh et al. (2000), but LPO because of the anisotropy of hcp iron is more likely. Ab initio calculations and experiments have provided elastic parameters, which are used to calculate the corresponding seismic velocities. The critical property is the *c/a* ratio, which determines the amount of anisotropy, where the *c*-axis is the cylindrical symmetry axis and the *a*-axis is perpendicular to it. *a* and *c* are related to the distances between noninteracting hard spheres packed in an hcp crystal lattice. For an ideal hcp iron crystal, the *c/a* ratio is 1.6229, which would make the crystal isotropic. At inner core pressure and ambient temperature, the *c/a* ratio is less than the ideal ratio, which makes the *c*-axis fast and the *a*-axis slow (Stixrude & Cohen 1995). The *c/a* ratio increases as a function of temperature, and some ab initio calculations suggested that it may become larger than the ideal value, making the *c*-axis slow and the *a*-axis fast instead (Steinle-Neumann et al. 2001, Gannarelli et al. 2005, Vočadlo et al. 2009). However, recent diamond anvil studies at inner core temperature and pressure all show that the *c/a* ratio for hcp is actually smaller than the ideal value. Thus, the *c*-axis is the fast axis and has to be aligned parallel to Earth's rotation axis to explain the seismically observed anisotropy.

The inner core consists of a large number of crystals, which will only appear to be anisotropic if they are aligned in the same direction. Two alternative regimes have been proposed: Either (*a*) the alignment is frozen in during the solidification process, or (*b*) deformation in the inner core leads to alignment after solidification.

7.2.1. Solidification texturing. In the solidification texturing regime, one possibility is that the alignment is with the magnetic field (Karato 1993) because of the paramagnetic properties of iron at inner core conditions. It is still unclear, however, whether the magnetic field would be strong enough to create alignment. In the alternative scenario, the inner core solidifies, creating dendritic structures aligned with flow in the outer core (Bergman 1997). For the *c*-axis to be aligned with the rotation axis, the outer core flow must extract more heat at the equator, which would result in the dendrites aligning in the equatorial plane. This model explains the increase in anisotropy with depth and the attenuation anisotropy seen with body waves.

7.2.2. Deformation texturing. In the deformation after solidification regime, there are three different mechanisms: (*a*) thermal convection (Jeanloz & Wenk 1988, Romanowicz et al. 1996), (*b*) Maxwell stress from Earth's magnetic field (Karato 1999, Buffett & Wenk 2001), or (*c*) preferential growth in the equatorial regions (Yoshida et al. 1996). Koot & Dumberry (2011) have recently estimated the inner core viscosity from Earth's nutation observations and found it to be as low as $2–7 \times 10^{14}$ Pa s, which makes viscous deformation in the inner core a very likely possibility.

The first mechanism, thermal convection (Jeanloz & Wenk 1988, Romanowicz et al. 1996), is unlikely if the thermal conductivity of the inner core is indeed as high as recently has been suggested

(Pozzo et al. 2012). Most likely, the inner core only convected early in its history (Buffett 2009, Cottaar & Buffett 2012), which would potentially explain the layered structure in the inner core, such as an innermost inner core. The second mechanism, deformation by the Maxwell stress of the magnetic field, produces toroidal-type flow, which, in the model of Buffett & Wenk (2001), aligns the *c*-axis parallel to the equator and cannot explain the seismic anisotropy in which the fast axis is the rotation axis. In the model by Karato (1999), the flow is axisymmetric and therefore able to align the *c*-axis with Earth's rotation axis. If inner core anisotropy is indeed due to Maxwell stress deformation, then a very exciting opportunity arises to link lateral and radial variations in inner core anisotropy to the magnetic field of the past.

The third and final mechanism, the model of Yoshida et al. (1996), argues that the inner core grows predominantly at the equator. As a consequence, axisymmetric flow toward Earth's poles keeps the inner core in hydrostatic equilibrium, aligning the *c*-axis parallel to the rotation axis to produce the seismic anisotropy. Several recent studies have extended this idea. For example, Deguen et al. (2011) add stable compositional stratification at the top of the inner core, which would lead to strong deformation and alignment in the upper inner core. The resulting anisotropy would be radial, which would appear isotropic to body waves and explain the isotropic layer at the top of the inner core. However, this version of the mechanisms cannot explain the deeper anisotropy of the inner core, which would have to be an inherited older structure, perhaps from solidification texturing or deformation because of the Maxwell stress.

In my opinion, we do not have a full understanding yet of what causes the inner core anisotropy. It is difficult to distinguish between the different regimes, and different mechanisms may operate at the same time, which would be especially important for explaining the variations in anisotropy with depth. For example, solidification texturing may create the structure just below the inner core boundary, but deformation deeper in the inner core may realign and overprint the original alignment in a different direction. Each of these mechanisms predicts a different relationship between the magnetic field at the inner core boundary, viscosity of the inner core or heat flow at the core-mantle boundary, and lateral variations in inner core structure and anisotropy. Thus the anisotropic and heterogeneous structure of the inner core provides the key to understanding the driving mechanism of the geodynamo and our magnetic field and the inner working of our planet. Most importantly, we need stronger constraints on inner viscosity to be able to distinguish between the different options in the future.

7.3. Hemispherical Structure

The main challenge in the dynamics of the inner core is explaining the origin of the hemispherical structure, in particular the existence of sharp boundaries between the hemispheres as well as stronger anisotropy, lower velocity, and less attenuation in the western hemisphere. Two scenarios have been proposed, but neither is able to explain all seismologically observed features.

7.3.1. Inner core translation. The inner core translation model was proposed to explain the existence of the F layer at the base of the outer core (Alboussière et al. 2010), which has a larger concentration of light elements. In this model, crystallization happens in the west and the east is melting, continually renewing the inner core on a timescale of approximately 100 Myr (Monnereau et al. 2010). Inner core translation is a mode of inner core convection, and it may not be happening if the thermal conductivity is indeed as high as recently suggested (Pozzo et al. 2012). Also, it requires an inner core viscosity of more than 10^{18} Pa s (Deguen 2012), which is several orders of magnitude larger than the value found from core nutation observations (Koot & Dumberry 2011).

The translating inner core model is proposed to result in different crystal sizes in the two hemispheres, which would explain the difference in isotropic velocity and attenuation between east and west (Monnereau et al. 2010). However, the translating inner core model does not explain the existence of anisotropy, and it requires another mechanism to create the texturing, such as the equatorial growth model of Yoshida et al. (1996). Annealing during the eastward translation would then remove the texture and make the eastern hemisphere less anisotropic (Bergman et al. 2010). The sharp hemisphere boundaries (Waszek et al. 2011, Waszek & Deuss 2011) pose another problem, especially as Monnereau et al. (2010) proposed a gradual transition between the hemispheres. However, a recent study showed that the translation model can actually result in sharp boundaries in the top of the inner core (Geballe et al. 2013). Finally, it would be difficult to explain the existence of the innermost inner core in this model, but superrotation would be compatible with the translation model as it does not require that the inner core be locked to the mantle.

7.3.2. Thermochemical flow. The idea in this model is that thermochemical convection in the outer core couples the variations in heat flow at the core-mantle boundary to inner core solidification (Sumita & Olson 1999). The thermochemical convection of the outer core results in a large cyclone under Asia (Aubert et al. 2008), which concentrates the magnetic field in one hemisphere, leading to asymmetric solidification at the inner core boundary. Solidification will be faster in the eastern hemisphere, leading to more randomly orientated dendrites (e.g., Bergman 1997) and thus less anisotropy, a higher velocity, and stronger attenuation, in agreement with the seismic observations. This model requires inner core superrotation to be less than 1°/Myr.

Alternatively, Gubbins et al. (2011) proposed that variations in mantle heat flow, coupled with the geodynamo flow in the outer core, result in regions at the inner core boundary that display localized melting. Again, melting explains the F layer and would be able to generate large-scale lateral variation such as the hemispheres. The thermal structure at the core-mantle boundary has probably remained the same for the past 100–300 Myr at least, which explains hemispherical variations in the upper 100–200 km of the inner core. In the thermochemical flow models, it is still unclear how to explain the deeper hemispherical variations and how the isotropic layer at the top of the inner core was formed.

The discussion of how to interpret the hemispheres and potentially link their existence to the solidification at the inner core boundary also raises the issue of time, especially the age of the inner core. The age of the inner core is still heavily debated in the current academic literature and depends on assumptions for values such as the heat flow at the core-mantle boundary, the presence or absence of radioactive heating, and the thermal conductivity of the inner core. Estimates for the age of the inner core vary from 0.6 to approximately 2 Gyr, suggesting that the inner core is much younger than Earth (see Nimmo 2007 for a recent review). Most estimations give values around 1 Gyr, which seems to be the accepted value at the moment. For this average age, the top 100 km would indeed have solidified in the past 100 Myr.

SUMMARY POINTS

1. The top 60–80 km of the inner core is isotropic, and the deeper parts have 3–4% anisotropy. The anisotropy exists in both velocity and attenuation; waves traveling in the polar direction are faster and more attenuated than waves traveling equatorially.
2. There may be an innermost inner core with different anisotropy, though evidence is not compelling.

3. The inner core displays a hemispherical variation: The western hemisphere is more strongly anisotropic, has a lower isotropic compressional velocity, and is less attenuating than the eastern hemisphere. There are sharp boundaries between the two hemispheres.
4. Inner core superrotation is less than 0.5°/yr and may even be as small as 0.1–1°/Myr.
5. Several mechanisms have been proposed to create the anisotropy and hemispherical structure of the inner core, but none of these mechanisms is yet able to explain all seismically observed features.

FUTURE ISSUES

1. Improved seismic images of the smaller-scale regional variations in inner core structure, including the hemispheres, are required, by installation of seismic stations and arrays near the polar regions. In addition, the larger-scale structure imaging using normal modes requires the continued operation of broadband seismometers capable of measuring seismic data at the millihertz frequency range.
2. Improved constraints on viscosity, reconciling the values found from different techniques, are essential to determine which dynamic mechanism may be responsible for the anisotropy of the inner core and its hemispherical variations.
3. Research on anisotropy and heterogeneity of the inner core has reached the stage that lithosphere research was in during the late 1950s and early 1960s. Numerous new data observations suggested ideas such as continental drift, but the discovery of plate tectonics was required to explain everything correctly. We need the discovery of the equivalent of plate tectonics for the inner core to explain all its recently observed features. So, these are exciting times for inner core research.

DISCLOSURE STATEMENT

The author is not aware of any affiliations, memberships, funding, or financial holdings that might be perceived as affecting the objectivity of this review.

ACKNOWLEDGMENTS

A.D. was funded by the European Research Council under the European Community's Seventh Framework Programme (FP7/2007–2013/ERC grant agreement 204995) and by a Philip Leverhulme Prize.

LITERATURE CITED

Alboussière T, Deguen R, Melzani M. 2010. Melting-induced stratification above the Earth's inner core due to convective translation. *Nature* 466:744–47

Andrews J, Deuss A, Woodhouse J. 2006. Coupled normal-mode sensitivity to inner-core shear velocity and attenuation. *Geophys. J. Int.* 167:204–12

Aubert J, Amit H, Hulot G, Olson P. 2008. Thermochemical flows couple the Earth's inner core growth to mantle heterogeneity. *Nature* 454:758–61

Aubert J, Dumberry M. 2011. Steady and fluctuating inner core rotation in numerical geodynamo models. *Geophys. J. Int.* 184:162–70

Aurnou J, Brito D, Olson P. 1998. Anomalous rotation of the inner core and the toroidal magnetic field. *J. Geophys. Res.* 103(B5):9721–38

Beghein C, Trampert J. 2003. Robust normal mode constraints on inner-core anisotropy from model space search. *Science* 299:552–55

Belonoshko AB, Ahuja R, Johansson B. 2003. Stability of the body-centred-cubic phase of iron in the Earth's inner core. *Nature* 424:1032–34

Bergman M. 1997. Measurements of electric anisotropy due to solidification texturing and the implications for the Earth's inner core. *Nature* 389:60–63

Bergman MI, Lewis DJ, Myint IH, Slivka L, Karato S, Abreu A. 2010. Grain growth and loss of texture during annealing of alloys, and the translation of Earth's inner core. *Geophys. Res. Lett.* 37:1–6

Bhattacharyya J, Shearer P, Masters G. 1993. Inner core attenuation from short-period *PKP(BC)* versus *PKP(DF)* waveforms. *Geophys. J. Int.* 114:1–11

Birch F. 1940. The alpha-gamma transformation of iron at high pressures, and the problem of the Earth's magnetism. *Am. J. Sci.* 238:192

Birch F. 1952. Elasticity and constitution of the Earth's interior. *J. Geophys. Res.* 57:227–86

Buffett BA. 1997. Geodynamic estimates of the viscosity of the Earth's inner core. *Nature* 388:571–73

Buffett BA. 2009. Onset and orientation of convection in the inner core. *Geophys. J. Int.* 179:711–19

Buffett BA, Huppert HE, Lister JR, Woods AW. 1992. Analytical models for solidification of the Earth's core. *Nature* 356:329–31

Buffett BA, Wenk H-R. 2001. Texturing of the Earth's inner core by Maxwell stresses. *Nature* 413:60–63

Bullen KE. 1946. A hypothesis on compressibility at pressures of the order of a million atmospheres. *Nature* 157:405

Bullen KE. 1951. Theoretical amplitudes of the seismic phase *PKJKP*. *Geophys. Suppl. MNRAS* 6:163–67

Cao A, Masson Y, Romanowicz B. 2007. Short wavelength topography on the inner-core boundary. *Proc. Natl. Acad. Sci. USA* 104:31–35

Cao A, Romanowicz B. 2004. Hemispherical transition of seismic attenuation at the top of the Earth's inner core. *Earth Planet. Sci. Lett.* 228:243–53

Cao A, Romanowicz B. 2007. Test of the innermost inner core models using broadband PKIKP travel time residuals. *Geophys. Res. Lett.* 34:L08303

Cao A, Romanowicz B, Takeuchi N. 2005. An observation of PKJKP: inferences on inner core shear properties. *Science* 308:1453–55

Collier J, Helffrich G. 2001. Estimate of inner core rotation rate from United Kingdom regional seismic network data and consequences for inner core dynamical behaviour. *Earth Planet. Sci. Lett.* 193:523–37

Cormier VF. 2007. Texture of the uppermost inner core from forward- and back-scattered seismic waves. *Earth Planet. Sci. Lett.* 258:442–53

Cormier VF, Attanayake J, He K. 2011. Inner core freezing and melting: constraints from seismic body waves. *Phys. Earth Planet. Inter.* 188:163–72

Cormier VF, Li X. 2002. Frequency-dependent seismic attenuation in the inner core. 2. A scattering and fabric interpretation. *J. Geophys. Res.* 107(B12):2362

Cormier VF, Stroujkova A. 2005. Waveform search for the innermost inner core. *Earth Planet. Sci. Lett.* 236:96–105

Côté AS, Vočadlo L, Brodholt JP. 2008. Light elements in the core: effects of impurities on the phase diagram of iron. *Geophys. Res. Lett.* 35:L05306

Cottaar S, Buffett B. 2012. Convection in the Earth's inner core. *Phys. Earth Planet. Inter.* 198–199:67–78

Creager KC. 1992. Anisotropy of the inner core from differential travel-times of the phases PKP and PKIKP. *Nature* 356:309–14

Creager KC. 1997. Inner core rotation rate from small-scale heterogeneity and time-varying travel times. *Science* 278:1284–88

Creager KC. 1999. Large-scale variations in inner core anisotropy. *J. Geophys. Res.* 104(B10):23127–39

Creager KC. 2000. Inner core anisotropy and rotation. In *Earth's Deep Interior: Mineral Physics and Tomography from the Atomic to the Global Scale*, ed. S Karato, A Forte, R Liebermann, G Masters, L Stixrude, pp. 89–114. Geophys. Monogr. Ser. 117. Washington, DC: AGU

Dahlen FA, Tromp J. 1998. *Theoretical Global Seismology*. Princeton, NJ: Princeton Univ. Press

Deguen R. 2012. Structure and dynamics of Earth's inner core. *Earth Planet. Sci. Lett.* 333–34:211–25

Deguen R, Cardin P, Merkel S, Lebensohn RA. 2011. Texturing in Earth's inner core due to preferential growth in its equatorial belt. *Phys. Earth Planet. Inter.* 188:173–84

Deuss A. 2008. Normal mode constraints on shear and compressional wave velocity of the Earth's inner core. *Earth Planet. Sci. Lett.* 268:364–75

Deuss A, Irving JCE, Woodhouse JH. 2010. Regional variation of inner core anisotropy from seismic normal mode observations. *Science* 328:1018–20

Deuss A, Ritsema J, van Heijst H. 2011. Splitting function measurements for Earth's longest period normal modes using recent large earthquakes. *Geophys. Res. Lett.* 38:L04303

Deuss A, Ritsema J, van Heijst H. 2013. A new catalogue of normal-mode splitting function measurements up to 10 mHz. *Geophys. J. Int.* 193:920–37

Deuss A, Woodhouse J. 2001. Theoretical free-oscillation spectra: the importance of wide band coupling. *Geophys. J. Int.* 146:833–42

Deuss A, Woodhouse J, Paulssen H, Trampert J. 2000. The observation of inner core shear waves. *Geophys. J. Int.* 142:67–73

Doornbos DJ. 1974. The anelasticity of the inner core. *Geophys. J. R. Astron. Soc.* 38:397–415

Dubrovinsky L, Dubrovinskaia N, Narygina O, Kantor I, Kuznetzov A, et al. 2007. Body-centered cubic iron-nickel alloy in Earth's core. *Science* 316:1880–83

Dumberry M. 2010. Gravitationally driven inner core differential rotation. *Earth Planet. Sci. Lett.* 297:387–94

Dumberry M, Mound J. 2010. Inner core-mantle gravitational locking and the super-rotation of the inner core. *Geophys. J. Int.* 181:806–17

Durek JJ, Romanowicz B. 1999. Inner core anisotropy inferred by direct inversion of normal mode spectra. *Geophys. J. Int.* 139:599–622

Dziewonski AM, Anderson DL. 1981. Preliminary reference Earth model. *Phys. Earth Planet. Inter.* 25:297–356

Dziewonski AM, Gilbert F. 1971. Solidity of the inner core of the Earth inferred from normal mode observations. *Nature* 234:465–66

Fearn D, Loper D, Roberts P. 1981. Structure of the Earth's inner core. *Nature* 292:232–33

Gannarelli C, Alfè D, Gillan M. 2005. The axial ratio of hcp iron at the conditions of the Earth's inner core. *Phys. Earth Planet. Inter.* 152:67–77

Garcia R. 2002. Constraints on upper inner-core structure from waveform inversion of core phases. *Geophys. J. Int.* 150:651–64

Garcia R, Souriau A. 2000. Inner core anisotropy and heterogeneity level. *Geophys. Res. Lett.* 27:3121–24

Garcia R, Tkalčić H, Chevrot S. 2006. A new global PKP data set to study Earth's core and deep mantle. *Phys. Earth Planet. Inter.* 159:15–31

Geballe ZM, Lasbleis M, Cormier VF, Day EA. 2013. Sharp hemisphere boundaries in a translating inner core. *Geophys. Res. Lett.* 40:1719–23

Glatzmaier G, Roberts PH. 1995. A three-dimensional convective dynamo solution with rotating and finitely conducting inner core and mantle. *Phys. Earth Planet. Inter.* 91:63–75

Gubbins D. 1981. Rotation of the inner core. *J. Geophys. Res.* 86(B12):11695–99

Gubbins D, Alfè D, Masters G, Price D, Gillan M. 2003. Can the Earth's dynamo run on heat alone? *Geophys. J. Int.* 155:609–22

Gubbins D, Sreenivasan B, Mound J, Rost S. 2011. Melting of the Earth's inner core. *Nature* 473:361–63

He X, Tromp J. 1996. Normal-mode constraints on the structure of the Earth. *J. Geophys. Res.* 101(B9):20053–82

Irving JCE, Deuss A. 2011a. Hemispherical structure in inner core velocity anisotropy. *J. Geophys. Res.* 116:B04307

Irving JCE, Deuss A. 2011b. Stratified anisotropic structure at the top of Earth's inner core: a normal mode study. *Phys. Earth Planet. Inter.* 186:59–69

Irving JCE, Deuss A, Woodhouse JH. 2009. Normal mode coupling due to hemispherical anisotropic structure in Earth's inner core. *Geophys. J. Int.* 178:962–75

Ishii M, Dziewonski A. 2002. The innermost inner core of the Earth: evidence for a change in anisotropic behavior at the radius of about 300 km. *Proc. Natl. Acad. Sci. USA* 99:14026–30

Ishii M, Dziewonski A. 2003. Distinct seismic anisotropy at the centre of the Earth. *Phys. Earth Planet. Inter.* 140:203–17

Ishii M, Dziewonski AM, Tromp J, Ekström, G. 2002a. Joint inversion of normal mode and body wave data for inner core anisotropy. 2. Possible complexities. *J. Geophys. Res.* 107(B12):2380

Ishii M, Tromp J, Dziewonski AM, Ekström G. 2002b. Joint inversion of normal mode and body wave data for inner core anisotropy. 1. Laterally homogeneous anisotropy. *J. Geophys. Res.* 107(B12):2379

Isse T, Nakanishi I. 2002. Inner-core anisotropy beneath Australia and differential rotation. *Geophys. J. Int.* 151:255–63

Ivan M, Marza V, Caixeta D, Arraes T. 2006. Uppermost inner core attenuation from PKP data observed at some South American seismological stations. *Geophys. J. Int.* 164:441–48

Jeanloz R, Wenk H-R. 1988. Convection and anisotropy of the inner core. *Geophys. Res. Lett.* 15:72–75

Jephcoat A, Olsen P. 1987. Is the inner core of the Earth pure iron? *Nature* 325:332–35

Julian BR, Davies D, Sheppard RM. 1972. PKJKP. *Nature* 235:317–18

Karato S. 1993. Inner core anisotropy due to the magnetic field–induced preferred orientation of iron. *Science* 262:1708–11

Karato S. 1999. Seismic anisotropy of Earth's inner core caused by Maxwell stress–induced flow. *Nature* 402:871–73

Kazama T, Kawakatsu H, Takeuchi N. 2008. Depth-dependent attenuation structure of the inner core inferred from short-period Hi-net data. *Phys. Earth Planet. Inter.* 167:155–60

Koot L, Dumberry M. 2011. Viscosity of the Earth's inner core: constraints from nutation observations. *Earth Planet. Sci. Lett.* 308:343–49

Koper KD, Dombrovskaya M. 2005. Seismic properties of the inner core boundary from PKiKP/P amplitude ratios. *Earth Planet. Sci. Lett.* 237:680–94

Koper KD, Pyle M. 2004. Observations of *PKiKP/PcP* amplitude ratios and implications for earth structure at the boundaries of the liquid core. *J. Geophys. Res.* 109:B03301

Krasnoshchekov DN, Kaazik PB, Ovtchinnikov VM. 2005. Seismological evidence for mosaic structure of the surface of the Earth's inner core. *Nature* 435:483–87

Laske G, Masters G. 1999. Limits on differential rotation of the inner core from an analysis of the Earth's free oscillations. *Nature* 402:66–69

Laske G, Masters G. 2003. The Earth's free oscillations and the differential rotation of the inner core. In *Earth's Core: Dynamics, Structure, Rotation*, ed. V Dehant, KC Creager, S Karato, S Zatman, pp. 5–22. AGU Geodyn. Ser. 31. Washington, DC: AGU

Lehmann I. 1936. P′. *Publ. Bur. Cent. Seismol. Int. A* 14:87–115

Li A, Richards P. 2003. Using earthquake doublets to study inner core rotation and seismicity catalog precision. *Geochem. Geophys. Geosyst.* 4:1072

Li X, Cormier V. 2002. Frequency-dependent seismic attenuation in the inner core. 1. A viscoelastic interpretation. *J. Geophys. Res.* 107(B12):2361

Lindner D, Song X, Ma P, Christensen DH. 2010. Inner core rotation and its variability from nonparametric modeling. *J. Geophys. Res.* 115:B04307

Lythgoe K, Deuss A, Rudge J, Neufeld J. 2013. Earth's inner core: innermost inner core or hemispherical variations? *Earth Planet. Sci. Lett.* 385:181–89

Mäkinen A, Deuss A. 2011. Global seismic body-wave observations of temporal variations in the Earth's inner core, and implications for its differential rotation. *Geophys. J. Int.* 187:355–70

Mäkinen A, Deuss A. 2013. Normal mode splitting function measurements of anelasticity and attenuation in the Earth's inner core. *Geophys. J. Int.* 194:401–16

Masters G, Gubbins D. 2003. On the resolution of density within the Earth. *Phys. Earth Planet. Inter.* 140:159–67

Masters G, Laske G, Gilbert F. 2000. Autoregressive estimation of the splitting matrix of free-oscillation multiplets. *Geophys. J. Int.* 141:25–42

McSweeney TJ, Creager KC, Merrill RT. 1997. Depth extent of inner-core anisotropy and implications for geomagnetism. *Phys. Earth Planet. Inter.* 101:131–56

Monnereau M, Calvet M, Margerin L, Souriau A. 2010. Lopsided growth of Earth's inner core. *Science* 328:1014–17

Mooney WD, Laske G, Masters G. 1998. CRUST5.1: a global crustal model at 5° × 5°. *J. Geophys. Res.* 103(B1):727–47

Morelli A, Dziewonski AM, Woodhouse JH. 1986. Anisotropy of the inner core inferred from *PKIKP* travel times. *Geophys. Res. Lett.* 13:1545–48

Nimmo F. 2007. Energetics of the core. In *Treatise on Geophysics*, Vol. 8: *Core Dynamics*, ed. P Olson, pp. 31–66. New York: Elsevier

Niu F, Chen Q-F. 2008. Seismic evidence for distinct anisotropy in the innermost inner core. *Nat. Geosci.* 1:692–96

Niu F, Wen L. 2001. Hemispherical variations in seismic velocity at the top of the Earth's inner core. *Nature* 410:1081–84

Niu F, Wen L. 2002. Seismic anisotropy in the top 400 km of the inner core beneath the "eastern" hemisphere. *Geophys. Res. Lett.* 29:1611

Okal EA, Cansi Y. 1998. Detection of *PKJKP* at intermediate periods by progressive multi-channel correlation. *Earth Planet. Sci. Lett.* 164:23–30

Oldham RD. 1906. The constitution of the interior of the Earth, as revealed by earthquakes. *Q. J. Geol. Soc.* 62:456–75

Oreshin S, Vinnik L. 2004. Heterogeneity and anisotropy of seismic attenuation in the inner core. *Geophys. Res. Lett.* 31:L02613

Ouzounis A, Creager K. 2001. Isotropy overlying anisotropy at the top of the inner core. *Geophys. Res. Lett.* 28:4331–34

Poupinet G, Pillet R, Sourriau A. 1983. Possible heterogeneity of the Earth's core deduced from PKIKP travel times. *Nature* 305:204–6

Poupinet G, Souriau A, Coutant O. 2000. The existence of an inner core super-rotation questioned by teleseismic doublets. *Phys. Earth Planet. Inter.* 118:77–88

Pozzo M, Davies C, Gubbins D, Alfè D. 2012. Thermal and electrical conductivity of iron at Earth's core conditions. *Nature* 485:355–58

Ritsema J, Deuss A, van Heijst HJ, Woodhouse JH. 2011. S40RTS: a degree-40 shear-velocity model for the mantle from new Rayleigh wave dispersion, teleseismic traveltime and normal-mode splitting function measurements. *Geophys. J. Int.* 184:1223–36

Romanowicz B, Breger L. 2000. Anomalous splitting of free oscillations: a re-evaluation of possible interpretations. *J. Geophys. Res.* 105(B9):21559–78

Romanowicz B, Li X, Durek J. 1996. Anisotropy in the inner core: Could it be due to low-order convection? *Science* 274:963–66

Sakai T, Ohtani E, Hirao N, Ohishi Y. 2011. Stability field of the hcp-structure for Fe, Fe-Ni, and Fe-Ni-Si alloys up to 3 Mbar. *Geophys. Res. Lett.* 38:L09302

Sharrock DS, Woodhouse JH. 1998. Investigation of time dependent inner core structure by the analysis of free oscillation spectra. *Earth Planets Space* 50:1013–18

Shearer PM. 1994. Constraints on inner-core anisotropy from *PKP(DF)* travel-times. *J. Geophys. Res.* 99(B10):19647–59

Shearer PM, Rychert CA, Liu Q. 2011. On the visibility of the inner-core shear wave phase *PKJKP* at long periods. *Geophys. J. Int.* 185:1379–83

Shearer PM, Toy KM. 1991. *PKP(BC)* versus *PKP(DF)* differential travel-times and aspherical structure in the Earth's inner core. *J. Geophys. Res.* 96(B2):2233–47

Singh SC, Taylor MAJ, Montagner JP. 2000. On the presence of liquid in the Earth's inner core. *Science* 287:2471–72

Song X. 2000. Joint inversion for inner core rotation, inner core anisotropy, and mantle heterogeneity. *J. Geophys. Res.* 105(B4):7931–43

Song X, Dai W. 2008. Topography of Earth's inner core boundary from high-quality waveform doublets. *Geophys. J. Int.* 175:386–99

Song X, Helmberger DV. 1995. Depth dependence of anisotropy of Earth's inner core. *J. Geophys. Res.* 100(B6):9805–16
Song X, Helmberger DV. 1998. Seismic evidence for an inner core transition zone. *Science* 282:924–27
Song X, Li A. 2000. Support for differential inner core superrotation from earthquakes in Alaska recorded at South Pole station. *J. Geophys. Res.* 105(B1):623–30
Song X, Poupinet G. 2007. Inner core rotation from event-pair analysis. *Earth Planet. Sci. Lett.* 261:259–66
Song X, Richards P. 1996. Seismological evidence for differential rotation of the Earth's inner core. *Nature* 382:221–24
Song X, Xu X. 2002. Inner core transition zone and anomalous PKP(DF) waveforms from polar paths. *Geophys. Res. Lett.* 29:1042
Souriau A. 1998. New seismological constraints on differential rotation of the inner core from Novaya Zemlya events recorded at DRV, Antarctica. *Geophys. J. Int.* 134:F1–5
Souriau A, Poupinet G. 2000. Inner core rotation: a test at the worldwide scale. *Phys. Earth Planet. Inter.* 118:13–27
Souriau A, Romanowicz B. 1996. Anisotropy in inner core attenuation: a new type of data to constrain the nature of the solid core. *Geophys. Res. Lett.* 23:1–4
Souriau A, Romanowicz B. 1997. Anisotropy in the inner core: relation between P-wave velocity and attenuation. *Phys. Earth Planet. Inter.* 101:33–47
Souriau A, Roudil P. 1995. Attenuation in the uppermost inner core from broad-band GEOSCOPE *PKP* data. *Geophys. J. Int.* 123:527–87
Souriau A, Souriau M. 1989. Ellipticity and density at the inner core boundary from subcritical PKiKP and PcP data. *Geophys. J. Int.* 98:39–54
Steinle-Neumann G, Stixrude L, Cohen R, Gulseren O. 2001. Elasticity of iron at the temperature of the Earth's inner core. *Nature* 413:57–60
Stixrude L, Cohen RE. 1995. High-pressure elasticity of iron and anisotropy of Earth's inner core. *Science* 267:1972–75
Stixrude L, Wasserman E, Cohen R. 1997. Composition and temperature of Earth's inner core. *J. Geophys. Res.* 102(B11):24729–39
Su WJ, Dziewonski AM. 1995. Inner-core anisotropy in three dimensions. *J. Geophys. Res.* 100(B6):9831–52
Su WJ, Dziewonski AM, Jeanloz R. 1996. Planet within a planet: rotation of the inner core of Earth. *Science* 274:1883–87
Sumita I, Olson P. 1999. A laboratory model for convection in Earth's core driven by a thermally heterogeneous mantle. *Science* 286:1547–49
Sun X, Song X. 2008. Tomographic inversion for three-dimensional anisotropy of Earth's inner core. *Phys. Earth Planet. Inter.* 167:53–70
Tanaka S. 2012. Depth extent of hemispherical inner core from PKP(DF) and PKP(Cdiff) for equatorial paths. *Phys. Earth Planet. Inter.* 210–211:50–62
Tanaka S, Hamaguchi H. 1997. Degree one heterogeneity and hemispherical variation of anisotropy in the inner core from *PKP*(BC)-*PKP*(DF) times. *J. Geophys. Res.* 102(B2):2925–38
Tateno S, Hirose K, Komabayashi T, Ozawa H, Ohishi Y. 2012. The structure of Fe-Ni alloy in Earth's inner core. *Geophys. Res. Lett.* 39:L12305
Tateno S, Hirose K, Ohishi Y, Tatsumi Y. 2010. The structure of iron in Earth's inner core. *Science* 330:359–61
Tkalčić H. 2010. Large variations in travel times of mantle-sensitive seismic waves from the South Sandwich Islands: Is the Earth's inner core a conglomerate of anisotropic domains? *Geophys. Res. Lett.* 37:L14312
Tkalčić H, Kennett BLN, Cormier VF. 2009. On the inner-outer core density contrast from PKiKP/PcP amplitude ratios and uncertainties caused by seismic noise. *Geophys. J. Int.* 179:425–43
Tkalčić H, Young M, Bodin T, Ngo S, Sambridge M. 2013. The shuffling rotation of the Earth's inner core revealed by earthquake doublets. *Nat. Geosci.* 6:497–502
Tomiyama K, Oda H. 2008. Estimation of inner-core rotation rate by using the Earth's free oscillation. *Acta Geophys.* 56:939–56
Tromp J. 1995. Normal-mode splitting due to inner-core anisotropy. *Geophys. J. Int.* 121:963–68
Tseng T, Huang B, Chin B. 2001. Depth-dependent attenuation in the uppermost inner core from the Taiwan short period seismic array PKP data. *Geophys. Res. Lett.* 28:459–62

Vidale JE, Dodge DA, Earle PS. 2000. Slow differential rotation of the Earth's inner core indicated by temporal changes in scattering. *Nature* 405:445–48

Vidale JE, Earle PS. 2000. Fine-scale heterogeneity in the Earth's inner core. *Nature* 404:273–75

Vidale JE, Earle PS. 2005. Evidence for inner-core rotation from possible changes with time in PKP coda. *Geophys. Res. Lett.* 32:L01309

Vinnik L, Romanowicz B, Breger L. 1994. Anisotropy in the center of the inner-core. *Geophys. Res. Lett.* 21:1671–74

Vočadlo L, Alfè D, Gillan M, Price G. 2003a. The properties of iron under core conditions from first principles calculations. *Phys. Earth Planet. Inter.* 140:101–25

Vočadlo L, Alfè D, Gillan M, Wood I, Brodholt J, Price G. 2003b. Possible thermal and chemical stabilisation of body-centred-cubic iron in the Earth's core. *Nature* 424:536–39

Vočadlo L, Brodholt J, Alfè D, Gillan MJ, Price GD. 2000. Ab initio free energy calculations on the polymorphs of iron at core conditions. *Phys. Earth Planet. Inter.* 117:123–37

Vočadlo L, Dobson DP, Wood IG. 2009. Ab initio calculations of the elasticity of hcp-Fe as a function of temperature at inner-core pressure. *Earth Planet. Sci. Lett.* 288:534–38

Vočadlo L, Wood IG, Alfè D, Price G. 2008. Ab initio calculations on the free energy and high P-T elasticity of face-centred-cubic iron. *Earth Planet. Sci. Lett.* 268:444–49

Waszek L, Deuss A. 2011. Distinct layering in the hemispherical seismic velocity structure of Earth's upper inner core. *J. Geophys. Res.* 116:B12313

Waszek L, Deuss A. 2013. A low attenuation layer in Earth's uppermost inner core. *Geophys. J. Int.* 195:2005–15

Waszek L, Irving J, Deuss A. 2011. Reconciling the hemispherical structure of Earth's inner core with its super-rotation. *Nat. Geosci.* 4:264–67

Wen L, Niu F. 2002. Seismic velocity and attenuation structures in the top of the Earth's inner core. *J. Geophys. Res.* 107(B11):2273

Woodhouse JH, Deuss A. 2007. Earth's free oscillations. In *Treatise on Geophysics*, Vol. 1: *Seismology and Structure of the Earth*, ed. B Romanowicz, A Dziewonski, pp. 31–65. New York: Elsevier

Woodhouse JH, Giardini D, Li X. 1986. Evidence for inner core anisotropy from free oscillations. *Geophys. Res. Lett.* 13:1549–52

Wookey J, Helffrich G. 2008. Inner-core shear-wave anisotropy and texture from an observation of PKJKP waves. *Nature* 454:873–76

Xu X, Song X. 2003. Evidence for inner core super-rotation from time-dependent differential PKP traveltimes observed at Beijing Seismic Network. *Geophys. J. Int.* 152:509–14

Yoshida SI, Sumita I, Kumazawa M. 1996. Growth model of the inner core coupled with the outer core dynamics and the resulting anisotropy. *J. Geophys. Res.* 101(B12):28085–103

Yu W, Wen L. 2006a. Inner core attenuation anisotropy. *Earth Planet. Sci. Lett.* 245:581–94

Yu W, Wen L. 2006b. Seismic velocity and attenuation structures in the top 400 km of the Earth's inner core along equatorial paths. *J. Geophys. Res.* 111:B07308

Yu W, Wen L. 2007. Complex seismic anisotropy in the top of the Earth's inner core beneath Africa. *J. Geophys. Res.* 112:B08304

Yu W, Wen L, Niu F. 2005. Seismic velocity structure in the Earth's outer core. *J. Geophys. Res.* 110:B02302

Zhang J, Richards PG, Schaff DP. 2008. Wide-scale detection of earthquake waveform doublets and further evidence for inner core super-rotation. *Geophys. J. Int.* 174:993–1006

Zhang J, Song X, Li Y, Richards P, Sun X, Waldhauser F. 2005. Inner core differential motion confirmed by earthquake waveform doublets. *Science* 309:1357–60